

**Proceedings**

**U.S.-JAPAN JOINT WORKSHOP  
AND  
THIRD GRANTEES MEETING**

**U.S.-JAPAN COOPERATIVE RESEARCH  
ON URBAN EARTHQUAKE DISASTER MITIGATION**

**Sponsored by**

**Monbu-Kagaku-sho and The National Science Foundation**

**15-16 August 2001**

**University of Washington, Seattle, Washington**

# VOID REDISTRIBUTION AND LOCALIZATION OF SHEAR STRAINS IN MODEL SAND SLOPES WITH SILT SEAMS: REPORT ON FIRST YEAR ACTIVITIES

Ramachandran Kulasingam  
Graduate Student

Department of Civil and Environmental Engineering, University of California, Davis  
Davis, CA 95616, USA ([rkulasingam@ucdavis.edu](mailto:rkulasingam@ucdavis.edu))

Erik J. Malvick  
Graduate Student

Department of Civil and Environmental Engineering, University of California, Davis  
Davis, CA 95616, USA ([ejmalvick@ucdavis.edu](mailto:ejmalvick@ucdavis.edu))

Ross W. Boulanger  
Associate Professor

Department of Civil and Environmental Engineering, University of California, Davis  
Davis, CA 95616, USA ([rwboulanger@ucdavis.edu](mailto:rwboulanger@ucdavis.edu))

Bruce L. Kutter  
Professor

Department of Civil and Environmental Engineering, University of California, Davis  
Davis, CA 95616, USA ([blkutter@ucdavis.edu](mailto:blkutter@ucdavis.edu))

## Abstract

Void redistribution due to pore pressure gradients associated with liquefaction has been identified as having a potentially significant effect on the shear resistance of saturated sands. Some results of an ongoing research project to investigate the role of void redistribution on the cyclic and post-liquefaction shear resistance behavior of sand are presented here. Nine models of sand slopes were shaken using the servo-hydraulic earthquake simulator on the 1 m radius centrifuge at the University of California, Davis. Eight of the model slopes included embedded silt seams, placed to impede drainage along a potential failure surface in the models. The results indicate that the void ratio sometimes increased below this relatively impermeable seam causing large localized shear strains below the seam. Some of the parameters found to influence the magnitude of localized shear strains are relative density, duration of shaking, volume change of soil beneath the impermeable layer, and seismic history. These and other influencing factors are discussed.

## Introduction

Laboratory testing by several investigators has shown that the shear resistance over a large range of strains is affected by stress path (extension vs. simple shear vs. compression), method of preparation, consolidation stress, fines content, and strain level. However, laboratory testing is not able to account for void redistribution driven by high pore pressures associated with liquefaction in the field. The residual or steady state strength of sands has long been known to be highly sensitive to the void ratio of the soil. Therefore, if void redistribution does occur, it will have an important influence on the shear resistance of saturated sands. The process of void redistribution within a globally undrained sand mass was termed Mechanism B by NRC (1985), and a potential situation where it might occur was illustrated by the schematic in Figure 1. Of related interest is Mechanism C (NRC 1985) where the outward flow of pore water due to excess pore pressures in a sand mass, such as illustrated in Figure 2, could spread into overlying soils and/or cause a loosening of the upper portion of the sand. In this case, the sand is neither globally nor locally undrained, since there is drainage from the sand.

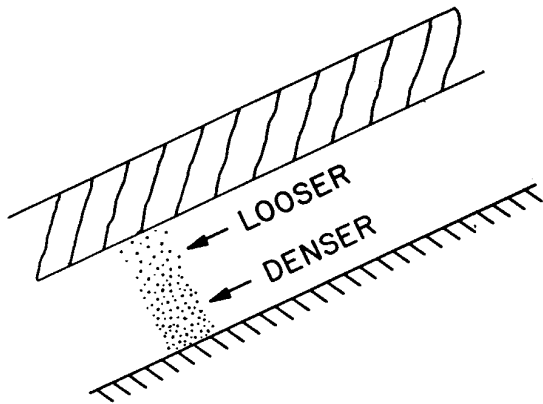


Figure 1. Mechanism B by NRC (1985)  
- Example of potential void redistribution within a globally undrained sand layer.

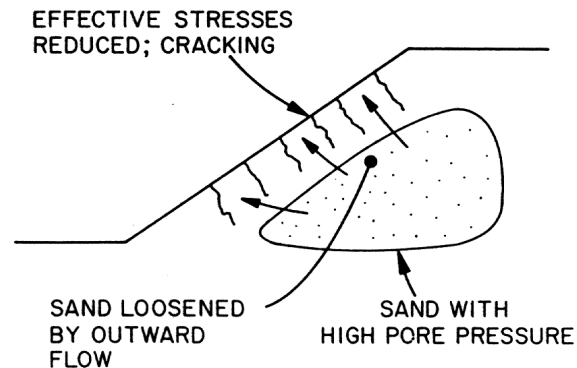


Figure 2. Mechanism C by NRC (1985) –  
Example of potential failure by spreading of excess pore pressures with global volume changes.

The primary objective of this paper is to investigate the role of void redistribution, which may be associated with impeded drainage or particle intermixing, on the liquefaction induced deformation of sand. Dynamic centrifuge model tests and laboratory triaxial tests are being conducted in collaboration with an ongoing program of 1-g shaking table tests by Professor Kokusho at Chuo University, Japan, to study this problem. Nine tests on the 1 m radius Schaevitz centrifuge at the University of California, Davis and one test on the 9 m radius National Geotechnical Centrifuge (NGC) have been completed in the first year of the project. In this paper, the results of the testing program completed on the Schaevitz centrifuge will be presented.

A unique asset of this project is a Board of Consultants (BOC) consisting of recognized experts in soil liquefaction to collaborate on the design and interpretation of the centrifuge experiments.

The members of the BOC are Dr. G. Castro and Professors R. Dobry, I. M. Idriss, T. Kokusho and S. L. Kramer. The BOC was included in this project due to the controversial nature of void redistribution effects, and their interaction has already made significant contributions to this project.

### Testing Program on the Schaevitz Centrifuge

A rigid model container with transparent side walls was used for all nine tests in the series. The inside dimensions of the container are 560 x 280 x 180 mm. Pore pressure transducers, accelerometers, and linear potentiometers were placed throughout the models to measure soil response. Up to 15 channels were used for data acquisition. The signals were amplified on-board and sent through slip rings to an off-board computer with an A/D converter.

All models primarily consisted of Nevada sand air pluviated to form an 8-m-tall, 1:2 (v:h) slope in the prototype scale. Because the centrifuge g-field is radial and these tests were performed on a small centrifuge, there is significant distortion of the geometry as indicated in Figure 3. Nevada sand is a uniform fine sand with a mean grain size of 0.14 mm. All models except one had a non-plastic silt arc (illustrated in Figure 3) of about 5 mm (model units) thickness in the slope. The silt arcs were constructed by placing the silt with a spoon and then lightly compacting the silt by static pressure from a standard 500 g mass. The mass resulted in vertical stresses of less than 5 kPa so that the soil was not overconsolidated under the in-flight stresses. Silica flour, which has a mean grain size of 0.02 mm, was used to form the silt arc. Nevada sand and the silt have approximate permeability values of  $5 \times 10^{-3}$  and  $3 \times 10^{-6}$  cm/s respectively (Fiegel & Kutter, 1994). A coarse Monterey sand layer was placed at the base of the container to aid saturation. A viscous solution of Hydroxypropyl methylcellulose (HPMC) in water was used as the pore fluid to compensate for the conflict between the time scale factors for dynamic and consolidation processes.

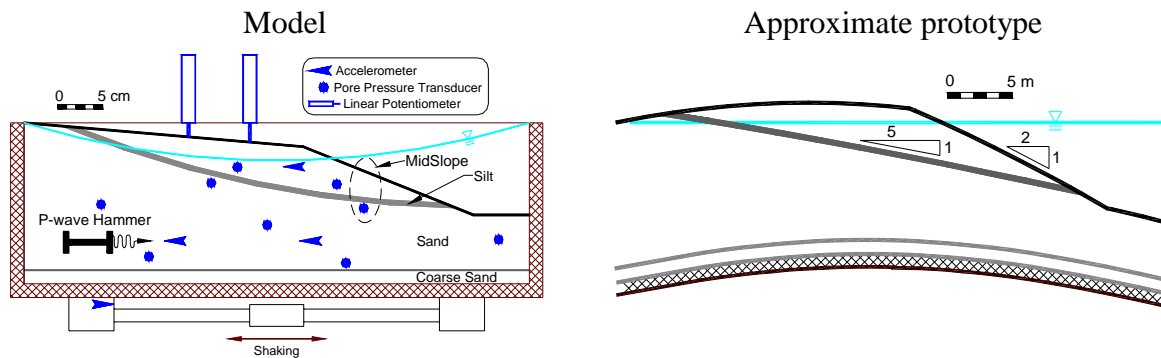


Figure 3. Illustration of centrifuge model geometry in model scale (left) and approximate prototype (right).

Models were spun to produce 80-g centrifugal accelerations in the model. Sufficient time was allowed for the pore pressures to build up and stabilize before shaking. In-flight P-wave velocity measurements were made to check the saturation of the models. The measurements were made using a source similar to the miniature air hammers described by Arulnathan et al. (2000) except

it was altered to produce P-waves. The P-waves are captured by two accelerometers aligned horizontally along the axis of the hammer and recorded using an oscilloscope.

Ground motions were applied at the base of the model parallel to the long sides of the container as indicated in Figure 3. Most of the models were subjected to more than one shaking event. After each shaking event, sufficient time was allowed for pore pressure dissipation and stabilization before spinning down. Photos were taken and the deformed models were usually spun up again and subjected to the next shaking event. After all shaking events were completed, the models were removed from the centrifuge arm and dissected.

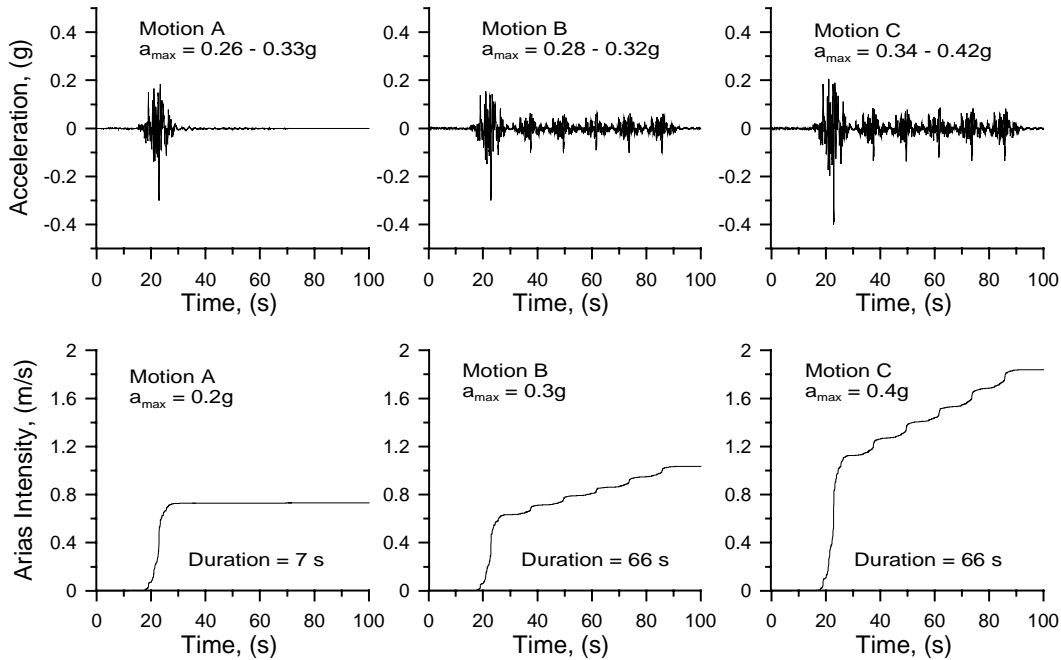


Figure 4. Input base motion time histories and Arias intensity plots for the base motions used in the testing program

As outlined in Table 1, parameters were varied for each test systematically to study the effect of soil density, shaking duration, shaking amplitude, shaking sequence, and volume of soil below the silt arc. The geometry of the slope and silt was the same for all the tests in this program. The pore fluid viscosity was kept at  $25 \pm 4$  cs for all the tests. Table 1 gives details of the testing program. Three different base motions were used for input and are shown in Figure 4. These motions are highly modified versions the ground motion recording at the UCLA grounds during the 1994 Northridge earthquake. Motion A (see Figure 4) was obtained by cutting off the lower intensity later part of the recorded motion to produce a short duration (7 sec), high intensity ground motion. This was done in an attempt to better differentiate between movements occurring during and after shaking. Motions B and C were prepared by adding an attenuated version of Motion A five times following the end of motion A.

Table 1. Testing program on Schaevitz centrifuge

Test No. (Name)	Relative density of Nevada sand (%)	Viscosity <sup>a</sup> (cs)	Geometry	P-wave velocity (m/s)	Base motion <sup>b</sup> [a <sub>max</sub> (g)]	Occurrence of concentrated strains <sup>c</sup>
1 (RKS03)	20	24	Nevada sand with underlying coarse sand	1190	Motion A (0.33)	No
2 (RKS04)	20	28	Silt arc in Nevada sand with underlying coarse sand No. 1	850	Motion A (0.29)	No
					Motion B (0.32)	Yes
3 (RKS05)	35	25	„	1130	Motion A (≈ 0.32)	No
					Motion B (≈ 0.32)	Yes
4 (RKS06)	70	28	„	840	Motion A (≈ 0.30)	No <sup>d</sup>
					Motion B (≈ 0.30)	No
					Motion C (≈ 0.34)	No
5 (RKS07)	55	23	„	450	Motion A (≈ 0.29)	No
					Motion B (≈ 0.29)	No
					Motion C (≈ 0.36)	No
6 (RKS08)	45	28	„	485	Motion A (≈ 0.26)	No
					Motion B (≈ 0.32)	No
					Motion C (≈ 0.40)	No
7 (RKS09)	30	29	„	1130	Motion A (0.32)	Yes
					Motion B (0.32)	Yes
8 (RKS10)	30	23	Silt arc in Nevada sand with underlying coarse sand No. 2 (lesser volume of sand below the silt arc)	680	Motion A (0.28)	No
					Motion B (0.28)	No
					Motion C (0.37)	No
9 (RKS11)	50	23	Silt arc in Nevada sand with underlying coarse sand No. 1	1200	Motion C (0.417)	Yes

<sup>a</sup>Viscosity of pore fluid determined per ASTM D 445 and D 2515.

<sup>b</sup>Models were subjected to one, two or three shaking events, separated by sufficient time for full dissipation of excess pore pressures between events. The shaking events are listed in their order of occurrence.

<sup>c</sup>Concentrated shear strains refers to the development of a shear zone beneath the silt arc, extending over more than one-half the silt arc length, and with local shear strains in excess of 100%.

<sup>d</sup>Concentrated shear strains occurred over a limited length near the toe of the slope, and with relative displacements of less than 0.25 m across the shear band, corresponding to maximum shear strains of about 60%.

## *Results of Test 2*

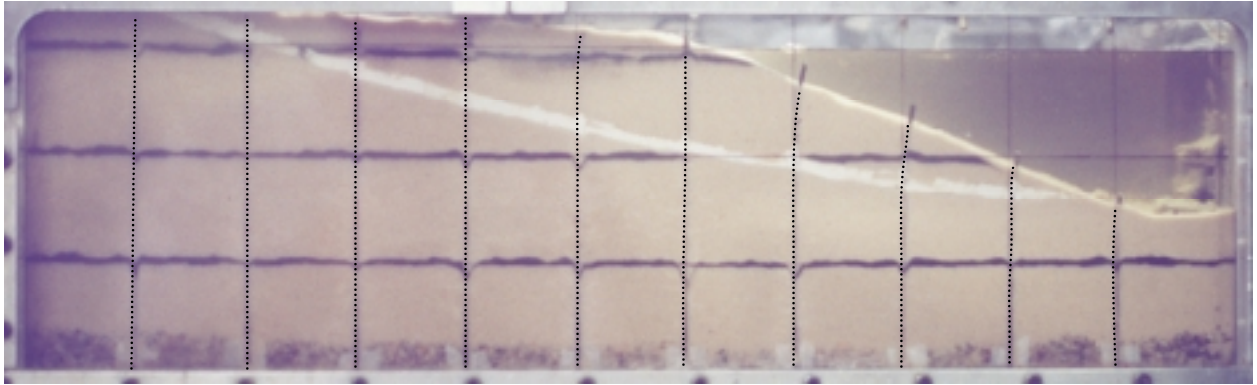
This model consisted of Nevada sand placed at an initial relative density of 20% with a silt arc embedded in the Nevada sand slope. The Nevada sand was underlain by a coarse sand drainage layer to facilitate saturation. A P-wave velocity of 850 m/s was measured for this test, indicating a reasonably high degree of saturation. Application of motion A (shaking event 1) did not result in the development of localized shear strains below the silt arc. Subsequently, motion B (shaking event 2) induced large slope movements and large localized shear strains below the silt arc.

Pre- and post- shaking event 1 (motion A) photos are shown as part of Figure 5. Significant shear strains were distributed along the height of the slope with approximate values ranging from about 15% in the sand above the silt arc to about 9% in the sand below the silt arc. These strains were measured at the mid-slope, and localization of shear strains was not observed. The maximum horizontal displacement at the top of mid-slope was 1.2 m. The accelerometer recordings indicate that there was no significant amplification of ground acceleration in the model. The pore pressure recordings show residual excess pore pressure ratios ranging from about 50% to 90% depending on the relative location to the slope. The linear potentiometer recording at the head part of the slope indicates that about 23% of the vertical settlements occurred after the end of shaking. A few silt boils appeared at the head part of the slope. A significant delay was observed between the end of the slope movements and the appearance of these boils.

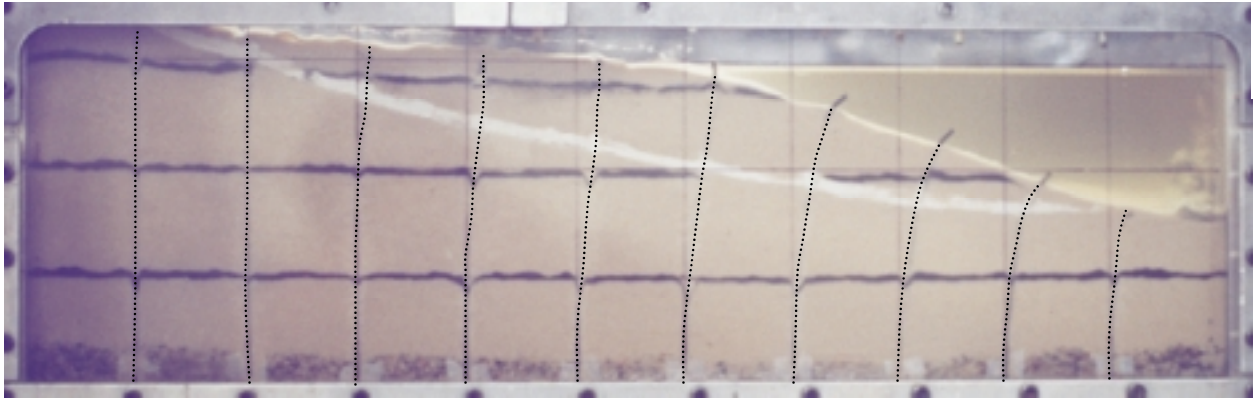
Pre- and post- shaking event 2 (motion B) photos are also shown as part of Figure 5. Large localized shear strains on the order of 200 - 400% in a thin zone immediately below the silt arc were observed in this shaking event. This resulted in an incremental displacement of 1.6 m across the shear zone at mid-slope. Shear strains were distributed in other parts of the slope with approximate increments due to shaking event 2 ranging from about 10% in the sand above the silt arc to about 5% in the sand below the silt arc. The incremental maximum horizontal displacement at the top of mid-slope due to shaking event 2 was 2.2 m. This brought the total horizontal displacement at the top of the mid-slope due to shaking events 1 and 2 to 3.4 m. These slope movements were constrained by the model container wall blocking the soil from moving further. Extensive silt boils and tension cracks were observed in the head part of the slope. There was a slight delay between the end of the slope movements and silt boil appearance. The pore pressure recordings indicate that even though the maximum pore pressures were almost the same as for shaking event 1, they remained high for a longer duration. The linear potentiometer recording near the head part of the slope indicates that 18% of the vertical settlements occurred after the end of shaking.

In all of the tests, horizontal colored sand layers and colored spaghetti noodles were placed vertically along the clear side walls of the container and used to visualize the deformation patterns. As desired, the spaghetti noodles became soft after soaking under water, but they also seemed to have some tendency to stretch, possibly limiting the resolution of the shear zone thickness that could be measured using the noodle markers.

Before Shaking:



After shaking event 1: Motion A,  $a_{\max}$  at the base = 0.29 g



After shaking event 2: Motion B,  $a_{\max}$  at the base = 0.32 g

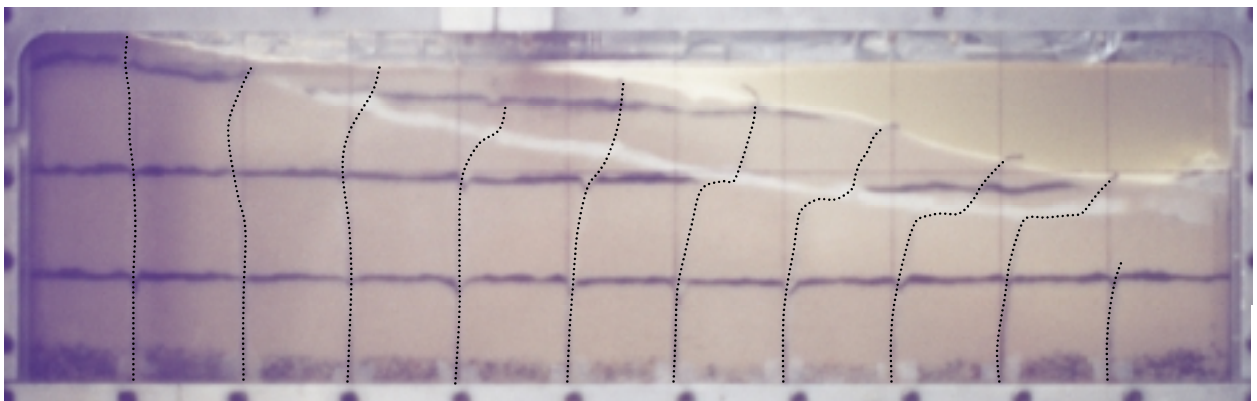


Figure 5. Photos from test 2 ( $D_r \approx 20\%$ , Sand with silt arc).

## Discussion

A series of centrifuge tests with the same geometry of the slope and silt arc and the same pore fluid viscosity were carried out. Other parameters were varied systematically. Some of the tests and shaking events produced large localized strains and large slope movements, whereas in other tests and shaking events deformations were smaller and localized strains were not produced. The large localized strains appear to occur in a thin zone of sand immediately below the silt arc and in the bottom part of the silt arc itself. It was not possible to determine whether the sand below the silt arc or the silt arc itself was the weakest link at the time of instability by visual inspection because of the stretching effect of the noodles as described before. It can be inferred that since the silt arc was placed in the same manner for all tests, the lack of localized strains in tests 4 to 6 suggest that the silt is not the weak point in the system. The lack of localized strains in the first shaking events of tests 2 and 3 add additional support to this claim. The instability was generated by the loosening of the dilating zone of sand immediately below the silt arc. This was caused by the low permeability layer retarding the drainage of the water flow driven by the liquefaction-induced hydraulic gradients. Coincidence of the shape of this loosened zone with a kinematically admissible failure mechanism defined by the silt arc resulted in large slope movements.

This series of tests increased our understanding of the effects of various parameters on the development of large localized strains and resulting large slope movements due to void redistribution. Some of the parameters thought to influence the amount of void redistribution are initial relative density, base motion duration, volume change of sand below the silt arc and shaking history.

### *Influence of Initial Relative Density*

Six of the models tested had the same slope geometry and sequence of shaking. These six tests (tests 2 – 7) had sand placed at different initial relative densities varying from 20% - 70%, and provide an opportunity to study the effect of initial relative density on the development of large localized strains and resulting large slope movements.

Figure 6 shows the influence of initial relative density on the cumulative maximum horizontal displacement at the mid-slope surface (from measurements of spaghetti noodles) for these six models. The location of the "mid-slope" surface is indicated in Figure 3. The slope movement measurements for this figure correspond to points just below the sand surface, and hence do not include any effects of shallow surface ravelling as was often observed. For comparison, the data from the sand model without a silt arc (test 1) is also shown. Motions A, B and C were applied as shaking events 1, 2 and 3 as explained before. It can be seen that the slope movements increase as initial relative density decreases. For this slope geometry and shaking sequence, there seems to be a critical relative density of about 35% below which, localization is observed. Motion C was not applied for tests with initial relative densities less than or equal to 35% because they already developed large slope movements during Motions A and B. Measurements of the incremental horizontal displacements across the shear zone at mid-slope revealed interesting information. When large localized strains occurred as a result of shaking with motion B (after A), the incremental horizontal displacements across the shear zone at mid-slope had a value of about roughly 1.6 m regardless of the initial relative density value. The uniform strains

in the sand below and above the silt arc increased as relative densities decreased. The maximum horizontal displacements at the mid-slope surface shown in Figure 6 are due to a combination of shear strains of a few percent throughout the slope and the much greater localized strains in the shear zone. For shaking with motion A, localized strains developed in only the 30% initial relative density case. For shaking with motion A, the larger movements for  $D_r = 30\%$  than for  $D_r = 20\%$  (see Figure 6) may be explained by differences in the degree of saturation, the ground motion intensity, errors in measurement of relative density, or other factors that are being explored further. As will be seen below, localized shear strains could also be produced in  $D_r = 50\%$  sand, depending on the seismic history.

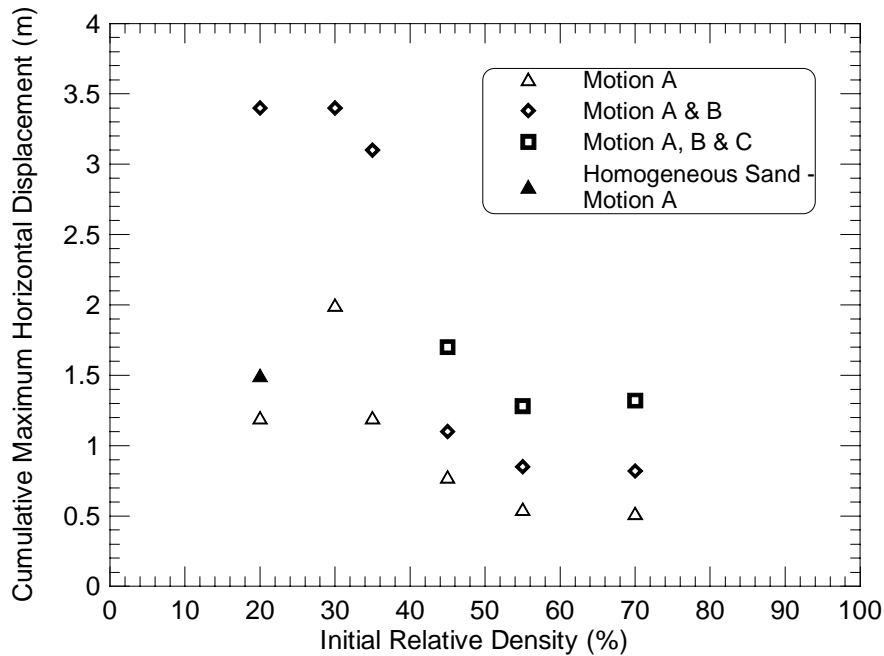


Figure 6. Influence of the initial relative density and base motion on cumulative maximum horizontal displacements at the mid-slope surface (surface raveling omitted)

### *Effect of Base Motion Duration*

The duration of the ground motion was found to be an important parameter influencing the occurrence of large localized shear strains. Large localized shear strains below the silt arc and resulting large slope movements were observed in shaking event 2 (Motion B) of tests 2, 3, and 7 and shaking event 1 (Motion C) of test 9. Note that in tests 2 and 3 the application of shorter duration motion A as shaking event 1 did not cause noticeable localized strains. In test 7 the application of motion A as shaking event 1 did cause localized shear strains to occur, but the movements were only half of those caused by the subsequent application of the longer duration motion B. Test 9 consisted of one shaking event with the application of motion C. Based on these results, longer duration motions are more likely to cause large localized strains than shorter duration motions. Longer duration motions with after shocks, like motions B and C, allow more water migration during the shaking event and greater potential for void redistribution.

### *Effect of Volume of Sand below the Silt Arc*

Models 7 and 8 had sand placed at 30% initial relative density, but with a different volume of soil below the silt arc. Model 7 was similar to the other models in this testing program with a 9 m soil height below the silt arc at mid-slope. Model 8 had only a 3 m soil height below the silt arc at mid-slope. Model 7 developed large localized strains and large slope movements during shaking event 1 (motion A) and shaking event 2 (motion B), whereas no localized strains developed in model 8 even after being subjected to three shaking events (motions A, B and C). The relative volumes of the dilating and contracting regions influences the amount of void redistribution. If the volume change of contracting soil is large compared to the volume of dilating soil, the potential for softening of the dilating soil is increased, favoring the formation of localized shear zones. A large volume of contracting soil generates a large amount of water that is expelled both during and after shaking. The volume change of the contracting soil will increase as the volumetric strain increases and as the volume of contracting soil increases.

### *Effect of Shaking Sequence*

Models 5 and 6 had sand placed at initial relative densities of 55% and 45% respectively. They were subjected to shaking with motions A, B and C in that order. Localized strains did not develop in either test due to these shaking events. Pore pressure records indicate that the soil became more resistant to pore pressure generation, likely due to densification during the seismic shaking history. Model 9 had sand placed at an initial relative density of 50%, intermediate to the two models described above. Motion C was used for the first shaking event for model 9. Large localized strains below the silt arc and large slope movements occurred due to this shaking event. This clearly shows the effect of shaking sequence on the amount of void redistribution and the resulting localized strains.

### *Other Factors*

Void redistribution induced instability of a layered slope is a complex coupled transient seepage boundary value problem. Many factors have the potential to influence the formation and development of localized shear zones. Some of these factors, in addition to those discussed above, that could possibly influence the amount of void redistribution, are the permeability contrast of the soils, maximum pore pressure ratio ( $r_{u,max}$ ) developed due to shaking, the thickness and shape of the low permeability layer, and the distance to the free draining boundaries from the low permeability layer. Tests from this testing program are not sufficient to draw any conclusions about the extent to which these parameters influence the void redistribution. Simplified analysis or more detailed numerical analysis based studies will be helpful in understanding the influence of these parameters on void redistribution.

### *Relating the Timing of Surface Deformations to the Mechanisms of Soil Behavior*

The results of these centrifuge experiments illustrate how difficult it is to relate the underlying mechanisms of soil behavior to the timing and magnitude of ground surface displacements. In simplified terms, slope deformations may be considered to develop due to cyclic mobility of the

soil (limited shear strains induced by the cyclic loading), flow instability if the soil reaches critical state under the imposed shear stresses, or additional shear and volumetric strains associated with the flow of pore water under the shaking-induced excess pore pressure gradients. Cyclic mobility only occurs during shaking. Flow instability may occur during or after shaking, with the timing potentially being affected by the timing of any void redistribution. Deformations due to pore water flow (or void redistribution), which may cause void ratio increases (such as below an impeded drainage boundary) or void ratio decreases (such as in contracting zones undergoing reconsolidation), can also occur during and after shaking. Therefore, the timing of ground surface displacements provides only limited guidance regarding the underlying mechanisms. If ground surface displacements develop mainly during shaking, the only conclusion that can be reached is that post-shaking contributions of void redistribution were relatively small. It does not mean that void redistribution did not contribute to the deformations during shaking. If large ground surface displacements develop mainly after shaking, the only conclusions that can be reached are that either (i) the shaking plus some amount of post-shaking creep was just sufficient to cause the liquefied soil to collapse toward critical state, (ii) post-shaking failure of non-liquefied portions of the slope contributed to the delay of deformations, or (iii) post-shaking void redistribution had a significant effect on the shear resistance of the liquefied soil. Consequently, observations of ground deformations in the field (e.g., “lateral spread” versus “flow failure”) and their timing provide only limited evidence as to the underlying mechanisms of soil behavior.

## Conclusions

- The dynamic centrifuge testing program to study the effect of void redistribution on liquefaction behavior of a sand slope with an embedded silt arc indicates that void redistribution induced localized shear strains and resulting large slope movements can take place under the combined presence of certain factors.
- Some parameters found to influence the amount of void redistribution include initial relative density, base motion duration, volume of sand below the silt arc, and shaking sequence.
- Some other factors that are likely to influence the amount of void redistribution are the permeability contrast of the soils, maximum pore pressure ratio ( $r_{u,max}$ ) developed due to shaking, the slope geometry (height, slope angle), and the soil stratigraphy (layer thickness, sequences and geometry).
- Future research, both experimental and computational, is needed to try and quantify the effects of void redistribution on liquefaction induced deformations and to enable the use of these research findings in design practice.

## Acknowledgments

This ongoing research project is funded by the National Science Foundation under grant CMS-0070111. The authors are very thankful to Dr. G. Castro and Professors R. Dobry, I. M. Idriss, T. Kokusho and S. L. Kramer for serving on the Board of Consultants for this project. The assistance of W. K. Sluis and D. A. Kehlet of the Department of Civil and Environmental Engineering, and Dr. D. W. Wilson, C. L. Justice, T. L. Coker and T. J. Kohnke from the Center for Geotechnical Modeling, UC Davis are greatly appreciated. Some initial

exploratory testing was performed in collaboration with B. Sunman (Sunman 2000) and the authors are very thankful for her contributions.

## References

- Arulnathan, R., Boulanger, R. W., Kutter, B. L., and Sluis, B. (2000). "New tool for shear wave velocity measurements in model tests." *Geotechnical Testing Journal*, GTJODJ, ASTM, 23(4): 444-453.
- Fiegel, G. L., and Kutter, B. L. (1994). "Liquefaction - induced lateral spreading of mildly sloping ground." *J. Geotech. Engrg.*, ASCE, 120(12), 2236 – 2243.
- National Research Council [NRC](1985). *Liquefaction of Soils During Earthquakes*. National Academy Press, Washington, D.C.
- Sunman, B. (2000). *Effects of Layering on Liquefaction – Induced Deformations in Submerged Slopes*. MSc thesis, Univ. of Calif., Davis, Calif.